THE JOURNAL OF PHYSICAL CHEMISTRY C

Article

pubs.acs.org/JPCC

A Capacitance Mediated Positive Differential Resistance Oscillator Model for Electrochemical Systems Involving a Surface Layer

Carla Zensen, Konrad Schönleber, Felix Kemeth, and Katharina Krischer*

Non-equilibrium Chemical Physics, Physik-Department, TU München, James-Franck-Strasse 1, 85748 Garching, Germany

ABSTRACT: We present a novel mechanism for potentiostatic current oscillations in systems involving the electrochemical formation and chemical dissolution of a surface layer on the electrode. The essential variables of the model are the capacitance of and the potential drop across the passive layer. Thus, they are both of electrical nature. We discuss the feedback loops destabilizing the stationary states and corroborate that the oscillations occur with an entirely positive faradaic impedance. Furthermore, it is demonstrated that the oscillations develop around a current plateau in a CV and that the model predicts superharmonic resonances in admittance spectra taken at a stable stationary state with oscillatory transients.

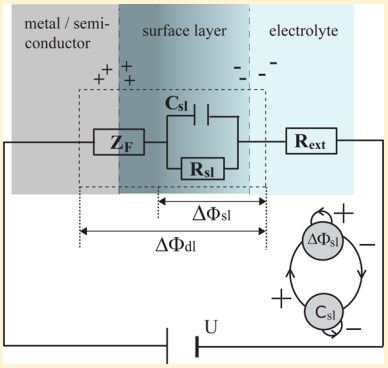

1. INTRODUCTION

Oscillations in electrochemical systems were discovered more than 150 years ago, and for at least the past 100 years they have attracted considerable interest. During the first half of the twentieth century especially studies on the oscillating electrodissolution of iron and other metal electrodes were conducted, motivated by the striking similarity of their oscillatory dynamics and potential waves occurring in nerve impulse propagation.[1−3] In the 1980s it was then discovered that also many electrocatalytic reactions exhibit oscillatory phenomena, and this without the participation of an oxide on the electrode surface.[4,5] Furthermore, the importance of a negative differential resistance (NDR) in the polarization curve for the oscillatory instability was recognized.[6] A deeper understanding of the oscillation mechanisms, however, came only in the early 1990s with the formulation of a general mathematical model for electrochemical systems with an N-shaped NDR in the stationary current-potential characteristic.[7] In the following decade, different types of NDRs with distinct dynamical properties were distinguished. This led to the nowadays established classification of electrochemical oscillators into essentially four types of oscillatory systems:[8−12]

- *N-NDR oscillators* possess an N-shaped stationary polarization curve. The oscillations require an ohmic resistance in series with the electrochemical interface, the electrode potential is the activatory variable, and typically the dynamic of the concentration of an electroactive species provides the negative feedback variable.
- In *HN-NDR systems* the N-shaped NDR is *hidden* in the stationary currrent-electrode potential curve by a slow electrochemical process, but at some finite frequency the interfacial impedance becomes real and negative. Also here, a finite series resistance is necessary for oscillations to occur and the electrode potential plays the role of the activator, the inhibitor variable being of a chemical nature and associated with the slow NDR hiding process. In contrast to N-NDR systems, HN-NDR systems exhibit also oscillations under galvanostatic conditions.
- *S-NDR systems* have an S-shaped, i.e., bistable, polarization curve. Here, only chemical species are involved in the positive feedback, the electrode potential acting as inhibitor in the presence of an ohmic series resistance. Those systems only oscillate under special conditions, e.g., when the effective area is particularly large, making the capacitance of the electrode large and thus slowing down the characteristic time of the inhibitor.[13]
- In *strictly potentiostatic oscillations* the electrode potential is a parameter, the oscillatory mechanism involving only chemical species.

Finally we note that, besides these four oscillator classes, a few further mechanisms are known which lead to oscillations, involving, e.g., gas bubble convection.[14−16] These mechanisms often also involve a negative differential resistance in the current-potential curve, but seem to be more specific to the respective system such that they are usually not listed in the general classification scheme summarized above.

Irrespective of this apparently comprehensive picture of electrochemical oscillators, there is one category of oscillatory electrochemical systems, which does not fall into one of the above-mentioned classes and for which the oscillation mechanism is still an active field of research. These are systems that involve the electrochemical oxidation of the electrode with successive film formation. There are a variety of electrode/electrolyte combinations belonging to this category, the two

Received: June 2, 2014
Revised: August 25, 2014
Published: September 22, 2014

dx.doi.org/10.1021/jp505418x | J. Phys. Chem. C 2014, 118, 24407−24414

most prominent examples being the electrodissolution of silicon in fluoride containing electrolytes at high anodic voltage, where the Si surface is covered by an oxide film (for a review on the many studies on this system see Chapter 5 in ref 17), and Fe dissolution in sulfuric acid at intermediate values of the applied voltage where an iron sulfate film precipitates on the electrode surface.[18−21] Note that these fast oscillations in the Fe system occur on a transport-limited current plateau and are to be distinguished from the activation-passivation oscillations close to the Flade potential, which are of the N-NDR-type. For both, the Fe and the Si systems different oscillatory mechanisms were suggested, involving, e.g., an ionic breakthrough of the Si oxide layer in the former system[22] or hydrodynamic transport or a viscous layer of low conductivity for the iron system.[18,19,21] Yet, the mechanisms are not generally accepted and cannot account for a number of experimental observations. Other examples of dissolving cover layer systems include the anodic oxidation of other semiconductor electrodes such as InP, GaP, or GaN.[23−25]

In the following, we present a general mechanism that might lead to oscillations in electrochemical systems involving the formation and dissolution of inhibiting surface layers. The essential variables of the model are of an electrical nature, yet, the current-voltage characteristic of the faradaic reaction does not possess an NDR. Moreover, in a CV, the oscillations occur on a current plateau, reflecting that with increasing driving force for the reaction and thus increasing surface layer thickness the current becomes eventually controlled by the ionic transport through the surface layer rather than by the electrochemical reaction. These properties apply to the systems in the last mentioned category of oscillators for which simple, mathematical mean field models are still missing, even in the cases where oscillation mechanisms were proposed. The objective of our work is to introduce a novel idea how oscillations in these systems may arise. Whether the mechanism holds for a particular system has to be validated in independent experiments. In this context, we would also like to stress that we do not suggest that all the mentioned systems with "plateau oscillations" follow necessarily the same mechanism.

In section 2 we discuss the base oscillator, i.e., a minimal model yielding oscillations. We start with a simple equivalent circuit and then first derive in general terms necessary conditions for the oscillatory instability to occur as well as the feedback loops involved. Then we scale the system to obtain a dimensionless mathematical model with a minimal number of parameters. This allows us to discuss the influence of the model parameters on the oscillatory region in a concise way. In section 3, we return to the physical formulation of the model and introduce extensions that make the system more realistic and alter the phenomenology of the oscillations considerably, but not the basic destabilizing mechanism or the role of the variables. This section is concluded with the discussion of the basic features of the cyclic voltammograms and admittance spectra predicted by the model. Section 4 summarizes the main findings and conclusions.

2. THE TWO-VARIABLE BASE OSCILLATOR

2.1. Equivalent Circuit and Destabilizing Feedback Loops. We consider a general electrodissolution reaction of a metal or semiconductor electrode and assume that the anodic oxidation reaction leads to some current-limiting surface layer on the electrode, such as an oxide or a salt layer. Furthermore, we assume that the layer is chemically dissolved at the oxide (salt)|electrolyte interface such that a dynamic equilibrium between the electrochemical formation and the dissolution rate of the surface layer can adjust. A typical example would be Si electrodissolution in an HF-containing electrolyte at high positive overvoltage.

In a simple approximation, the equivalent circuit shown in Figure 1A represents such an electrodissolution system. The

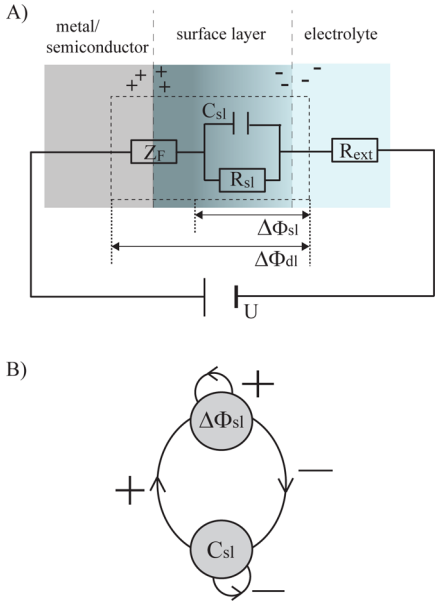

Figure 1. (A) Equivalent circuit of the electrochemical interface of interest. The dashed line frames the circuit elements that describe the base oscillator mechanism. (B) Feedback loops in the two-variable base oscillator.

centerpiece for our consideration is the parallel connection between the capacitor with a time-dependent capacitance $C_{sl}(t)$ and the ohmic resistor R_{sl}. It represents the current flow through the cover layer. The capacitive pathway takes into account that the cover layer may store (ionic) charges. A charge distribution across the entire interface as indicated in Figure 1A has been reported for Si electrodissolution.[26] Thus, in our model, the cover layer has a rather defective structure and some charge, which is generated in the faradaic reaction taking place at the metal (semiconductor)|cover layer interface, can be "trapped" in the oxide, e.g., in surface states or defect vacancies. The electronic defects are assumed to be generated by the oxidation current and to heal with time. Z_F represents the faradaic impedance of the oxidation reaction. The voltage drops across the entire interface and across the surface layer are denoted by $\Delta\phi_{dl}$ and $\Delta\phi_{sl}$, respectively. Finally, the resistor R_{ext} in series with the described interfacial impedance allows for some electrolyte resistance or other external ohmic resistors in series with the electrochemical interface, and U represents the voltage applied to the cell in a potentiostatic experiment.

Let us first restrict our considerations to the evolution equations of $\Delta\phi_{sl}$ and C_{sl} which contain the essential feedback loops that may render the steady state unstable. For the former the following expression is obtained from Kirchhoff's law applied to the minimal equivalent circuit indicated by dashes in Figure 1A:

$$\dot{\Delta\phi}_{sl} = \frac{1}{C_{sl}}\cdot\left(J_{ox} - \frac{\Delta\phi_{sl}}{R_{sl}}\right) - \frac{\dot{C}_{sl}}{C_{sl}}\cdot\Delta\phi_{sl} \quad (1)$$

where J_{ox} is the faradaic oxidation current. The last term on the rhs accounts for the fact that a larger capacitance accommodates a given charge already at a lower potential drop. Thus, an increasing capacitance leads to a decrease of $\Delta\phi_{sl}$ and vice versa. The time evolution of the capacitance $C_{sl}(t)$ is assumed to be proportional to the corresponding time evolution of the density of defects and surface states in the surface layer which offer binding sites where ions or partial charges can reversibly bind. This time evolution of the defect density is then in turn related to the oxidation current J_{ox} reflecting the idea that a layer formed far away from equilibrium, i.e., at higher J_{ox}, is expected to be more defective than a layer formed closer to equilibrium. Due to restructuring or relaxing of the surface layer, the defects or surfaces states are then assumed to heal or decay with a certain rate κ^- after they were created. Under these assumptions the time evolution of the surface layer capacitance is given by

$$\dot{C}_{sl} = \kappa^+\cdot J_{ox} - \kappa^-\cdot C_{sl} \quad (2)$$

where the constant κ^+ reflects the simple case of a proportional dependence of defect production rate on the oxidation current. Note that eq 2 implies an inhomogeneous layer structure perpendicular to the interface.

In order to illustrate that this base model may become oscillatory, we consider the linearized evolution equations

$$\begin{pmatrix} \delta\dot{\Delta\phi}_{sl} \\ \delta\dot{C}_{sl} \end{pmatrix} = \tilde{A}|_{ss}\begin{pmatrix} \delta\Delta\phi_{sl} \\ \delta C_{sl} \end{pmatrix} = \begin{pmatrix} a_{11} & a_{12} \\ a_{21} & a_{22} \end{pmatrix}\Bigg|_{ss}\begin{pmatrix} \delta\Delta\phi_{sl} \\ \delta C_{sl} \end{pmatrix} \quad (3)$$

where $\delta\Delta\phi_{sl}$ and δC_{sl} denote small perturbations from the steady state $(\Delta\phi_{sl}^{ss}, C_{sl}^{ss})$ in $\Delta\phi_{sl}$ and C_{sl}, respectively, and $\tilde{A}|_{ss}$ is the Jacobian matrix evaluated at the steady state $(\Delta\phi_{sl}^{ss}, C_{sl}^{ss})$:

$$\tilde{A}|_{ss} = \begin{pmatrix} \frac{1}{C_{sl}}\left[\frac{\partial J_{ox}}{\partial\Delta\phi_{sl}} - \frac{1}{R_{sl}} - \kappa^+\frac{\partial J_{ox}}{\partial\Delta\phi_{sl}}\Delta\phi_{sl}\right] & \frac{1}{C_{sl}}\kappa^- \\ \kappa^+\frac{\partial J_{ox}}{\partial\Delta\phi_{sl}} & -\kappa^- \end{pmatrix}\Bigg|_{ss} \quad (4)$$

Let us next look at the signs of the elements of the Jacobian matrix. For the oxidation current it is natural to assume that the current increases monotonically with the potential drop across the faradaic impedance Z_F, which is equal to $U - \Delta\phi_{sl}$ with U equaling $\Delta\phi_{dl}$ since we neglect an ohmic series resistance R_{ext} for the moment. In other words the quasi-stationary current-potential curve $J_{ox}(U - \Delta\phi_{sl})$ has a positive differential resistance throughout. Then, under potentiostatic control, J_{ox} decreases with increasing potential drop across the oxide, $\Delta\phi_{sl}$, and $(\partial J_{ox})/(\partial\Delta\phi_{sl}) < 0$. Hence, the first and the second term of a_{11} are always negative, but the third term is positive and may render a_{11} positive. Therefore, the dynamcis of $\Delta\phi_{sl}$ can become autocatalytic, the positive feedback being linked to the increase of C_{sl} with increasing current: A small perturbation $\delta\Delta\phi_{sl}$ of the steady state toward larger values prompts a smaller faradaic current, and therefore, also the generation rate of C_{sl} is smaller than in the steady state. The latter, however, causes a further increase in the potential drop across the oxide, $\Delta\phi_{sl}$, amplifying the original small perturbation. Thus, for appropriate parameter values, $\Delta\phi_{sl}$ is an autocatalytic variable, the positive feedback loop requiring a *positive* differential resistance of the quasi-static current-potential curve, $J_{ox}(U - \Delta\phi_{sl})$.

The signs of the other three elements of the Jacobian matrix $\tilde{A}$ can be seen easily. a_{12} is always positive and depends only on the decay rate of C_{sl}, reflecting the first order decay kinetics of C_{sl} and a production rate independent of C_{sl}. Thus, a capacitance of the surface layer slightly larger than the steady state value leads to a higher decay rate and thus an *increase* of $\Delta\phi_{sl}$. In other words, the positive sign in a_{12} mirrors the fact that C_{sl} activates the production of $\Delta\phi_{sl}$. C_{sl} is therefore an activatory variable.

a_{21} and a_{22} are both always negative, independent of the values of the parameters. From a physical point of view, the negative sign of a_{21} reflects the fact that the faradaic current decreases with increasing $\Delta\phi_{sl}$, which, according to our picture, leads to a surface layer with fewer defects. Thus, the production rate of C_{sl} becomes smaller, or is *inhibited* by a larger value of $\Delta\phi_{sl}$. We can therefore identify $\Delta\phi_{sl}$ as an inhibitor. Finally, the negative sign of a_{22} is due to the first order decay rate of C_{sl}. This feedback scheme is illustrated in Figure 1B.

In summary, eqs 1 and 2 may lead to the following sign scheme of the Jacobian matrix:

$$\operatorname{sgn}\tilde{A} = \begin{pmatrix} + & + \\ - & - \end{pmatrix} \quad (5)$$

which is characteristic of an activator−inhibitor system of "second type",[27] where the positive feedback variable, in our case $\Delta\phi_{sl}$, is the inhibitor and not the activator, as encountered in the majority of activator−inhibitor systems, and also in all electrochemical oscillator models mentioned above.

2.2. Dimensionless Model. For the further mathematical analysis we have to specify how the current depends on the potential drop across the reaction impedance $U - \Delta\phi_{sl}$. For our general considerations, a natural choice is to assume an exponential dependence

$$J_{ox} = K\ e^{f\cdot(U-\Delta\phi_{sl})} \quad (6)$$

with a reaction rate constant K and $f = 19.5\ V^{-1}$. Furthermore, we bring the system of eqs 1 and 2 in dimensionless form. Therefore, we introduce the following scalings:

$$x = \frac{\Delta\phi_{sl}}{K\ e^{fU}R_{sl}}; \quad y = \frac{C_{sl}}{C_{sl}^{av}}; \quad \tau = \frac{t}{R_{sl}C_{sl}^{av}} \quad (7)$$

where C_{sl}^{av} is an "average" or "typical" capacitance of the surface layer. The evolution equations for the dimensionless potential drop over the surface layer, x, and the dimensionless layer capacitance, y, then read

$$\dot{x} = \frac{1}{y}(k(x) - x) - \frac{\dot{y}}{y}x$$
$$\dot{y} = a_1 k(x) - a_2 y \quad (8)$$

where the dot over the variables x and y now denotes the first derivative with respect to τ and the dimensionless current density $k(x)$ is given by

$$k(x) = e^{-bx} \quad (9)$$

The dynamics depends on three parameters, the dimensionless formation and decay rate constants of the capacitance a_1 and a_2, respectively, and b, a dimensionless rate constant of the faradaic

dx.doi.org/10.1021/jp505418x | J. Phys. Chem. C 2014, 118, 24407−24414

reaction, which incorporates the voltage dependence of the current:

$$a_1 = \kappa^{+} R_{sl} K\, e^{fU}$$

$$a_2 = \kappa^{-} R_{sl} C_{sl}^{av}$$

$$b = f R_{sl} K\, e^{fU}$$

The system of eqs 8 has a stationary state at

$$(x_{ss}, y_{ss}) = \left(e^{-b x_{ss}}, \frac{a_1}{a_2} x_{ss} \right)$$

For appropriate values of the parameters, the steady state is unstable, any trajectory approaching a stable limit cycle. Oscillatory time series of x and y are shown in Figure 2A.

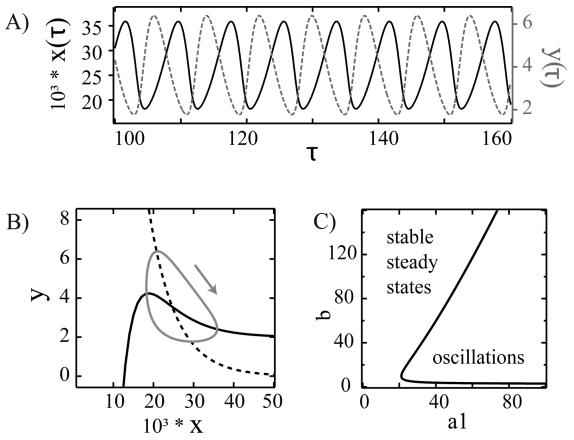

Figure 2. Dynamics of the dimensionless two-variable model eqs 8. (A) Time series for $a_1 = 75$, $a_2 = 0.5$, and $b = 150$. (B) Nullclines for x (solid) and y (dashed) and limit cycle for the parameters of A. (C) Hopf bifurcation line in the a_1−a_2 parameter plane.

Figure 2B depicts the nullclines of x (solid curve) and y (dashed curve) together with the stable limit cycle in phase space. Note that, independent of the values of the parameters, the nullclines have always only one intersection, excluding the occurrence of bistability in the system, as well as saddle loop or sniper (saddle node of infinite period) bifurcations. In fact, it can be easily shown that the oscillations emerge in a Hopf bifurcation. At a Hopf bifurcation, trace and determinant of the Jacobian fulfill the following conditions:

$$\mathrm{tr}\, \tilde{A}|_{ss} = 0 \quad \text{and} \quad \det \tilde{A}|_{ss} > 0 \tag{10}$$

The Jacobian of eqs 8 evaluated at the stationary state is given by

$$\tilde{A}|_{ss} = \begin{pmatrix} a_2 b x_{ss} - \dfrac{a_2}{a_1}\left(b + \dfrac{1}{x_{ss}}\right) & \dfrac{a_2^{\,2}}{a_1} \\ -b a_1 x_{ss} & -a_2 \end{pmatrix} \tag{11}$$

Thus, the conditions for the occurrence of a Hopf bifurcation translate to

$$x_{ss}^{\,2} - \left(\frac{1}{a_1} + \frac{1}{b}\right) \cdot x_{ss} - \frac{1}{a_1 b} = 0 \quad \text{and}$$

$$x_{ss} + \frac{1}{b} > 0 \tag{12}$$

We observe that both relations are independent of a_2 and that the second condition is always true since all variables and parameters are positive, confirming that the system has no saddle points. The first condition provides an analytic relation for the two bifurcation parameters a_1 and b. In Figure 2C, the Hopf bifurcation line is visualized in the a_1−b plane using the bifurcation analysis program *AUTO*.[28] Above a critical value of a_1, the system is oscillatory in an interval of b values which increases with increasing a_1. Recalling the physical meaning of the parameters a_1 and b, one can deduce that the system oscillates for sufficiently large formation rate constants of the capacitance, i.e., in our picture a suffficiently large production rate of defects or surface states that might accumulate charge, the oscillatory region in U being the broader the larger this formation constant is. In contrast, the healing rate a_2, or κ^{-}, sets the time scale of the oscillations, i.e., it is the main parameter determining the period of the oscillations.

Now we incorporate the effect of a series resistance R_{ext} on the oscillations in the two-variable model eq 8. Therefore, we replace $k(x)$ (eq 9) with the implicit expression.

$$k_R(x) = e^{-b(b_R k_R(x) + x)} \tag{13}$$

where the dimensionless external series resistance

$$b_R = \frac{R_{ext}}{R_{sl}}$$

acts as a fourth parameter. The Jacobian evaluated at the stationary state $x_{ss,R}$ reveals the influence of b_R:

$$\tilde{A}|x_{ss,R} = \begin{pmatrix} \dfrac{a_2 b x_{ss,R}}{1 + b b_R} - \dfrac{a_2}{a_1}\dfrac{1}{1 + b b_R} - \dfrac{a_2}{a_1 x_{ss,R}} & \dfrac{a_2^{\,2}}{a_1} \\ -\dfrac{b_1 a_1 x_{ss,R}}{1 + b b_R x_{ss,R}} & -a_2 \end{pmatrix} \tag{14}$$

For $b_R = 0$, the Jacobian given in eq 11 is retained. Furthermore, the sign matrix eq 5 is retained: For suitable values of a_2, b, and b_R, a_{11} can become positive, while a_{12} is always positive and the other two matrix elements are negative, independently of the parameter values. However, we also observe that the external series resistance decreases the magnitude of a_{11}, while leaving that of a_{22} unaffected. We can thus expect that the oscillations persist in the presence of an external series resistance, the oscillatory region in the a_1−b plane being, however, smaller than without an additional series resistance. This conjecture could be verified in simulations, which showed that limit cycle oscillations persist when incorporating the additional series resistance in model eqs 1, 2, but upon increasing the value of R_{ext} the oscillations die in a Hopf bifurcation. This result is also intuitive from a physical point of view: The decrease of the voltage $U - \Delta\phi_{sl}$ upon an increase in $\Delta\phi_{sl}$ is now shared between the voltage drop across Z_F and R_{ext}, which attenuates the above-described autocatalytic feedback loop.

dx.doi.org/10.1021/jp505418x | J. Phys. Chem. C 2014, 118, 24407−24414

3. MODEL EXTENSIONS AND PREDICTIONS

So far, we presented a minimal model for current oscillations in electrodissolution reactions of electrodes that lead to current-limiting surface layers and analyzed the physical origin of the feedback loops essential for the oscillatory behavior. In this section we demonstrate that the properties of the oscillations, such as oscillation amplitudes or shapes, depend strongly on the properties of the specific system and might exhibit widely varying features, even though the destabilizing mechanism of the stationary states stays always the same. This can be seen best when considering physical rather than dimensionless quantities. We therefore return in the following sections to the dimensional differential eqs 1 and 2 and the full equivalent circuit shown in Figure 1. This includes a series resistance R_{ext} so that the expression for the oxidation current becomes implicit and reads

$$J_{ox} = K\, e^{f(U-\Delta\Phi_{sl}-R_{ext}\cdot J_{ox})} \tag{15}$$

As already laid out in the last section for the dimensionless model, this additional series element does not cause qualitative changes of the oscillator mechanism (cf. eqs 13 and 14).

3.1. Oscillations of the Thickness of the Surface Layer. Since the surface cover layer is produced by the oscillating oxidation current, its thickness will also oscillate in general. Assuming the simplest case of a constant etching rate, ν_{etch}, the temporal changes of the thickness $\xi(t)$ of the layer can be readily obtained from

$$\dot{\xi} = \eta\cdot J_{ox} - \nu_{etch} \tag{16}$$

where $\eta = (M_{sl}/\rho)(1/AF\nu)$ with M_{sl} being the molar weight of the molecules forming the surface layer and ρ its density; A, F, and ν are the electrode area, Faraday's constant, and the number of electrons transferred in the oxidation reaction, respectively. η, thus, transforms the electrical current to a growth rate of the thickness of the surface layer. If the density of the porous cover film is not known, instead of the layer thickness its mass density per unit area $\tilde{\xi} = \xi\cdot\rho$ can be likewise determined, which is more easily accessible in experiments.

At this point, our considerations lead to two important conclusions. First, oscillations in the thickness of the surface layer, as reported in many experiments,[26,29−34] do not imply that the layer thickness is an independent degree of freedom of the system. In our model, they simply follow the dynamics of the oxidation current J_{ox}. Second, for a constant etch rate, the phase of the thickness oscillations lags $\pi/2$ behind the current oscillation. Such a phase relation, which was indeed found for the oscillation during Si electrodissolution in fluoride containing electrolytes,[26,33,35,36] suggests strongly that the oxide thickness (or mass density) is slaved to the oxidation current.

3.2. Feedback of the Layer Thickness on the Layer Resistance. In the following we assume that the resistance of the surface layer depends linearly on the layer thickness, and is thus given by

$$R_{sl}(t) = \rho_{sl}\cdot\xi(t) \tag{17}$$

with ρ_{sl} being the layer resistivity per unit area and $\xi(t)$ as above the thickness of the surface layer. Its dynamics is given by eq 16, the system of equations consisting now of eqs 1, 2, and 15−17.

The simulated time series of the oxidation current and the three variables are shown in Figure 3. Introducing the coupling

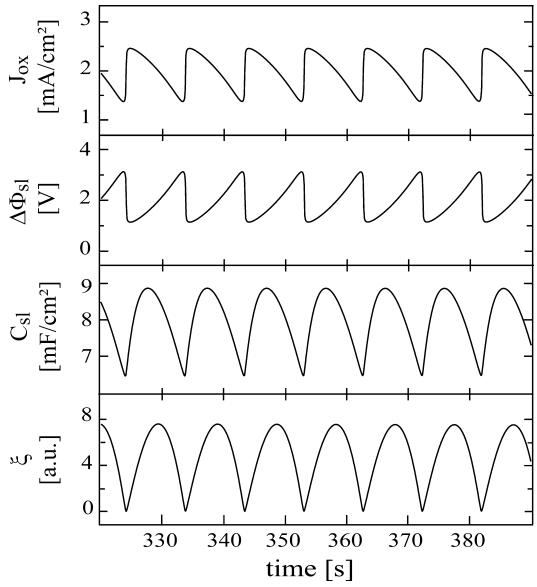

Figure 3. Simulated time series of the three variable model eqs 1, 2, and 15−17. Top panel: current density J_{ox}. Upper middle panel: surface layer potential $\Delta\phi_{sl}$. Lower middle panel: area specific capacitance C_{sl}. Bottom panel: layer thickness ξ. (Parameter values: U = 8 V, R_{ext} = 1.8 kΩ cm², ρ_{sl} = 0.8 kΩ cm², κ^{+} = 2 V^{-1}, κ^{-} = 0.5 s^{-1}, $K = 0.04\epsilon_0$ mA/(cm²·C), J_{etch} = 2 mA/cm², η = 5 cm³/(mA·s).

of the dynamics of the layer thickness to that of $\Delta\phi_{sl}$ changes the properties of the oscillations significantly in comparison to the time series of the base oscillator shown in Figure 2: The shape of the surface layer potential drop $\Delta\Phi_{sl}$ oscillations (and so the current oscillations) becomes less symmetric and more relaxation-like. In consequence (cf. eq 2), the oscillations of the surface capacitance show a very rapid sign reversal of the slope in their minima. The lowermost panel reveals that the thickness of the surface layer becomes periodically negligible. In this simple model, the latter is actually a characteristic feature of the oscillations. This breakdown of the layer facilitates its rapid discharge, and thus a decrease of $\Delta\phi_{sl}$ at finite current density and only slightly decreased values of C_{sl}. The breakdown of the surface layer causes a fast current rise. In reaction, the cover layer is regenerated and the dynamics follows again the base oscillator mechanism until the next breakdown occurs.

It is important to realize that these significant changes in the phenomenology of the oscillations do not affect the origin of the essential feedback loops, nor does it have an influence on the relative phases of current and layer thickness oscillations. The latter is still slaved to the current, and the oscillatory instability is caused by the interactions between activator−inhibitor variables as discussed above (cf. Figure 1B). Yet, a more quantitative description clearly requires to incorporate the temporal changes in the thickness of the layer in the model. Here, we only incorporated the impact of the layer thickness on its resistance. It is as well conceivable that also the capacitance of the cover layer depends on its thickness, in the simplest form according to $C_{sl} = \epsilon\epsilon_0\cdot A/\xi$, with ϵ and ϵ_0 being the dielectric constant and the vacuum permittivity, respectively. Equation 2 would then become an equation for ϵ. We refrain from investigating this effect on the oscillatory dynamics here since it is just one of several possible further dependencies that might be necessary to introduce when describing a specific electrochemical system. Rather, below we focus on general features of the base oscillator to characterize those properties that should

dx.doi.org/10.1021/jp505418x | J. Phys. Chem. C 2014, 118, 24407−24414

be independent of the detailed dynamics of the nonessential variables.

3.3. Cyclic Voltammetry. Cyclic voltammetry is an important tool to characterize an electrochemical reaction. Introducing a constant sweep rate ν_{sweep} of the externally applied voltage U,

$$\dot{U} = \nu_{sweep} \tag{18}$$

the three variable system eqs 1, 2, and 16 with J_{ox} and R_{sl} given by eqs 15 and 17 can be used to calculate a cyclic voltammogram (CV). Figure 4 shows such a simulated CV in the voltage range between 6.1 and 8 V together with changes of the layer thickness during the voltage scan. While ξ grows for increasing U, the current response stays on a plateau on average and is quasi-stationary during the forward sweep while it becomes oscillatory on the backward scan. While oscillations tend to occur more easily at large values of U, the onset potential and the maximum amplitude of current and thickness can be tuned in a wide range with the simulation parameters. Furthermore, the oscillations are not confined to the backward scan but can also start during the forward scan. This is expected because oscillations exist also under potentiostatic conditions and the system is not bistable.

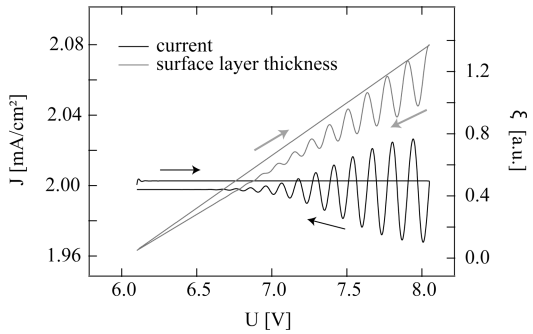

Figure 4. Simulated cyclic voltammogram and corresponding layer thickness variations for the three variable model eqs 1, 2, and 16 with a scan speed of ν_{scan} = 20 mV/s. (Parameter values: R_{ext} = 1.8 kΩ cm^2, ρ_{sl} = 0.8 kΩ cm^2, κ^+ = 2.0 V^{-1}, κ^- = 0.5 s^{-1}, $K = 0.04e_0$ mA/(cm^2·C), J_{etch} = 2 mA/cm^2, η = 5 cm^3/(mA·s).)

The described characteristic features of the simulated CV in Figure 4 differ strongly from those of oscillatory systems with an NDR, which are typically around a branch with increasing current or systems with an HN-NDR, which oscillate around a branch with increasing current. However, as mentioned in the Introduction, when the oxidation of the electrode leads to the buildup of an oxide or salt layer on the electrode, oscillations are frequently observed around a current plateau. Figure 4 demonstrates that the proposed oscillator offers a possible explanation of such oscillations. Whether it is in fact operative has to be tested for each specific system individually.

3.4. Impedance Spectroscopy. Impedance spectroscopy is another important technique to characterize processes at electrified interfaces. We calculated admittance spectra of stable stationary states of the two-variable base model (eqs 1, 2, 6) and of the three-variable full system (eqs 1, 2, 15−17) for different distances to the Hopf bifurcation. Therefore, the external applied voltage was modulated with a sinusoidal signal of small amplitude according to

$$U(t) = U_0(1 + 0.001\cdot\sin(\omega t)) \tag{19}$$

Parameters were chosen such that the stationary state was a stable focus, and special care was taken to impose the modulation of the voltage only after the system had settled to the stationary state.

Calculated admittance spectra are displayed in Figure 5. Figure 5A was obtained with the base model and Figure 5B−D with the three-variable model. All spectra exhibit unusual resonances. The highest peak is always found at approximately the natural frequency of the model and is close to the frequency of the damped oscillations in the current transient. Superharmonic resonances occur in both models. They are of a "shark fin" shape which is characteristic for the response of a resonant system on an oscillatory excitation.[37] When the Hopf bifurcation is approached (Figure 5B−D), more superharmonic resonances appear. This can be interpreted in the sense that the oscillations can already be "felt" in the "shadow" of a Hopf bifurcation.

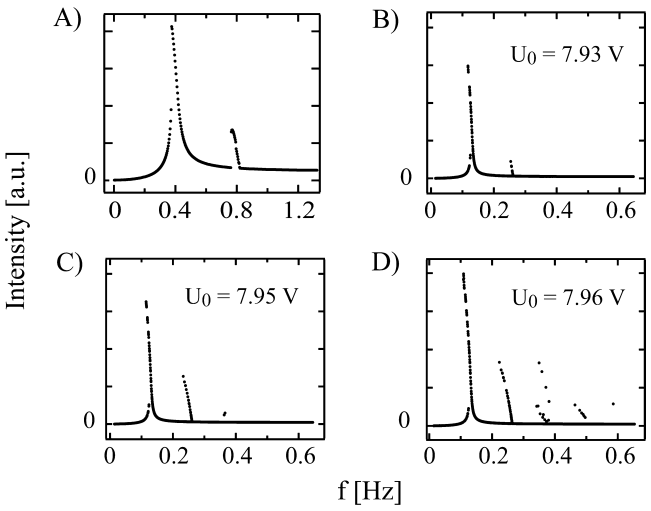

Figure 5. Admittance spectra in the vicinity of a Hopf bifurcation at U_H (oscillations for $U > U_H$) for (A) the base oscillator without an external resistance (eqs 1, 2) and (B−D) the three-variable model (eqs 1, 2, 15−17. (Parameter values: (A) base oscillator, U_0 = 3.745 V, R_{ext} = 0 kΩ cm^2, R_{sl} = 0.2 kΩ cm^2, κ^+ = 0.8 V^{-1}, κ^- = 0.5 s^{-1}, $K = 0.2e_0$ mA/(cm^2·C), U_H = 3.749 V; (B−D) three variable model, parameters of Figure 3, U_H = 7.975 V, the voltage U_0 is given separately in each plot.

In experiments, superharmonic resonances in admittance spectra were reported for the electrodissolution of Si in fluoride containing electrolyte.[38,39] Just as in our simulations, these spectra were obtained for voltage values at which the system exhibited damped oscillations. The authors interpreted the damped oscillations as well as the superharmonic resonances in the impedance spectra as a result of the interaction of many oscillating microdomains with a certain frequency distribution. According to this view, the damped oscillations are a result of the desynchronization of the microdomains, while the superharmonic resonances are caused by the frequency distribution of the oscillators. Figure 5 reveals that there is an alternative explanation for the data, namely, that the system is spatially uniform and close to a Hopf bifurcation. While the occurrence of superharmonic resonances in admittance spectra is likely to be characteristic for all electrochemical systems close to a Hopf bifurcation, it is interesting to note that the experimental system in which it was observed is one of the systems in which the oscillations might follow the mechanism proposed here.

dx.doi.org/10.1021/jp505418x | J. Phys. Chem. C 2014, 118, 24407−24414

Characteristic for the Si system is the wide voltage range in which oscillatory transients are found. This is different from other electrochemical oscillators which usually do not show oscillatory transients without a series resistance. Impedance spectra, on the other hand, are typically recorded under conditions under which any series resistance is minimized.

4. CONCLUSIONS

We derived a skeleton model for current oscillations in electrodissolution systems that form a current-limiting film on the electrode surface. The crucial idea of the model is that some charge can be stored in the otherwise resistive cover layer, and that the charge storage capacity changes with time. Accordingly, the capacitance of the film is an essential variable of the model. The repercussion of temporal changes of the capacitance on the potential drop across the surface layer, $\Delta\phi_{sl}$, the second essential variable, is responsible for the autocatalytic feedback of $\Delta\phi_{sl}$, as well as the activating (or positive) feedback of the capacitance on $\Delta\phi_{sl}$.

This "capacitance oscillator" does not fall into one of the established oscillator classes listed in the Introduction. The oscillations exist without an additional ohmic series resistance in the circuit and are not linked to a negative differential resistance or, in more general terms, a negative faradaic impedance, two prerequisites N-NDR, HN-NDR, or S-NDR systems must fulfill. But also the classification as a truly potentiostatic oscillator is problematic since the existence of the surface layer allows for the variation of the potential drop across the faradaic impedance, and the essential variables are of an electrical rather than a chemical nature, which is the case for the known strictly potentiostatic oscillators. From this point of view, it seems intuitive to classify the oscillator introduced here as a capacitance mediated positive differential resistance (C-PDR) oscillator.

As for diagnostic criteria, the following features are characterisic for a C-PDR-system and distinct from the different systems with an NDR; their experimental detection is thus a strong hint for the existence of a C-PDR system: (a) Oscillations occur around a current plateau in CVs and in relevant parameter regions there is no hint to the existence of bistability in CVs; (b) for certain parameter values, the oscillations exist without an ohmic resistance in series to the interface; and (c) in time series of current and layer thickness, the current maximum should preceed the cover layer maximum.

Several experimental, oscillating electrode dissolution reactions indeed meet at least criterion (a), some of them showing also other features reported for our model, for others it is not yet known wether the criteria hold or not. The similarities between the model and some experiments make it likely that the model is a step forward toward the understanding of oscillations in some anodic electrodissolution reactions. However, we also emphasize that the simple formulation of the complex physical processes in the surface layer presented here will not be sufficient to satisfyingly model any of the experimental systems quantitatively. We also demonstrated how sensitive amplitudes and shapes of the oscillations depend on model modifications. Thus, this work should be seen as a contribution of a possible oscillation mechanism in electrochemical systems. It is a challenge for future work to corroborate whether the underlying mechanism is indeed operative in any of the envisaged experimental systems.

AUTHOR INFORMATION

Corresponding Author

*E-mail: krischer@ph.tum.de.

Notes

The authors declare no competing financial interest.

ACKNOWLEDGMENTS

The authors thank Kazuhiro Fukami (Kyoto University) for fruitful discussions and acknowledge financial support from the Deutsche Forschungsgemeinschaft (Grant No. KR1189/12-1), and the cluster of excellence Nanosystems Initiative Munich (NIM).

REFERENCES

(1) Heathcote, H. L. Vorlaeufiger Bericht ueber die Passivitaet und Aktivierung des Eisens. *Z. Phys. Chem.* **1901**, *37*, 368−373.
(2) Bonhoeffer, K. F.; Renneberg, W. Ueber die Aktivitaetswellen auf passiven Eisendraehten. *Z. Phys.* **1941**, *118*, 389−400.
(3) Franck, U. Uber Die Aktivierungsausbreitung auf passiven Eisenelektroden. *Z. Elektrochem.* **1951**, *55*, 154−160.
(4) Horányi, G.; Visy, C. Potential Oscillations in the Course of Galvanostatic Oxidation of Hydrogen at Platinum Electrode in the Presence of Electrosorbing Cations. *J. Electroanal. Chem.* **1979**, *103*, 353−361.
(5) Hachkar, M.; Beden, B.; Lamy, C. Oscillating Electrocatalytic Systems: Part I. Survey of Systems Involving the Oxidation of Organics and Detailed Electrochemical Investigation of Formaldehyde Oxidation on Rhodium Electrodes. *J. Electroanal. Chem.* **1990**, *287*, 81−98.
(6) De Levie, R. On the Electrochemical Oscillator. *J. Electroanal. Chem. Interfacial Electrochem.* **1970**, *25*, 257−273.
(7) Koper, M. The Theory of Electrochemical Instabilities. *Electrochim. Acta* **1992**, *37*, 1771−1778.
(8) Koper, M. Non-linear Phenomena in Electrochemical Systems. *J. Chem. Soc.* **1998**, *94*, 1369−1378.
(9) Krischer, K. In *Modern Aspects of Electrochemistry*; Conway, B. E., Bockris, J. O., White, R., Eds.; Kluwer Academic/Plenum: New York, 1999; Vol. *32*, pp 1−142.
(10) Strasser, P.; Eiswirth, M.; Koper, M. T. Mechanistic Classification of Electrochemical Oscillators—An Operational Experimental Strategy. *J. Electroanal. Chem.* **1999**, *478*, 50−66.
(11) Krischer, K. New Directions and Challenges in Electrochemistry—Spontaneous Formation of Spatiotemporal Patterns at the Electrode Vertical Bar Electrolyte Interface. *J. Electroanal. Chem.* **2001**, *501*, 1−21.
(12) Krischer, K. In *Advances in Electrochemical Sciences and Engineering*; Kolb, D., Alkire, R., Eds.; Wiley-VCH: 2003; Vol. *8*, p 89.
(13) Kirsch, S.; Hanke-Rauschenbach, R.; El-Sibai, A.; Flockerzi, D.; Krischer, K.; Sundmacher, K. The S-Shaped Negative Differential Resistance during the Electrooxidation of H(2)/CO in Polymer Electrolyte Membrane Fuel Cells: Modeling and Experimental Proof. *J. Phys. Chem. C* **2011**, *115*, 25315−25329.
(14) Li, Z. L.; Cai, J. L.; Zhou, S. M. Potential Oscillations During the Reduction of Fe(CN)(6)(3-) Ions with Convection Feedback. *J. Electroanal. Chem.* **1997**, *432*, 111−116.
(15) Mukouyama, Y.; Nakanishi, S.; Konishi, H.; Ikeshima, Y.; Nakato, Y. New-type Electrochemical Oscillation Caused by Electrode-Surface Inhomogeneity and Electrical Coupling As Well As Stirring Through Electrochemical Gas Evolution Reaction. *J. Phys. Chem. B* **2001**, *105*, 7246−6253.
(16) Mukouyama, Y.; Kikuchi, M.; Okamoto, H. Appearance of New Potential Oscillation During Hydrogen Evolution Reaction by Addition of Na2SO4 and K2SO4. *J. Electroanal. Chem.* **2008**, *617*, 179−184.
(17) Zhang, X. G. *Electrochemistry of Silicon and its Oxides*; Kluwer Academic: 2001.

(18) Russell, P.; Newman, J. Anodic Dissolution of Iron in Acidic Sulfate Electrolytes I. Formation and Growth of a Porous Salt Film. *J. Electrochem. Soc.* **1983**, *130*, 547.
(19) Teschke, O.; Soares, D. M.; Kleinke, M. U. Colloidal Iron Sulfate Layer Formation and Breakdown as a Source of Current Oscillations. *Langmuir* **1989**, *5*, 1162−1169.
(20) Geraldo, A. B.; Barcia, O. E.; Mattos, O. R.; Huet, F.; Tribollet, B. New Results Concerning the Oscillations Observed for the System Iron−Sulphuric Acid. *Electrochim. Acta* **1998**, *44*, 455−465.
(21) Sazou, D.; Pagitsas, M. On the Onset of Current Oscillations at the Limiting Current Region Emerged During Iron Electrodissolution in Sulfuric Acid Solutions. *Electrochim. Acta* **2006**, *51*, 6281−6296.
(22) Foell, H.; Leisner, M.; Cojocaru, A.; Carstensen, J. Self-Organization Phenomena at Semiconductor Electrodes. *Electochim. Acta* **2009**, *55*, 327−339.
(23) Langa, S.; Carstensen, J.; Tiginyanu, I.; Christophersen, M.; Foell, H. Self-induced Voltage Oscillations During Anodic Etching of n-InP and Possible Applications for Three-Dimensional Microstructures. *Electrochem. Solid State Lett.* **2001**, *4*, G50−G52.
(24) Wloka, J.; Lockwood, D. J.; Schmuki, P. High Intensity and Oscillatory Electroluminescence Observed During Porous Etching of GaP in HBr and HF Electrolytes. *Chem. Phys. Lett.* **2005**, *414*, 47−50.
(25) Schaefer, S.; Wyrzgol, S. A.; Lercher, J. A.; Stutzmann, M.; Sharp, I. D. Charge Transfer across the GaN/Pt Nanoparticle Interface in an Electrolyte. *ChemCatChem* **2013**, *5*, 3224−3227.
(26) Chazalviel, J. N. Ionic Processes Through the Interfacial Oxide in the Anodic-Dissolution of Silicon. *Electrochim. Acta* **1992**, *37*, 865−875.
(27) Murray, J. *Mathematical Biology II*; Springer: 1989.
(28) Software for Continuation and Bifurcation Problems in Ordinary Differential Equations, http://indy.cs.concordia.ca/auto/. E. Doedel.
(29) Lewerenz, H. Anodic Oxides On Silicon. *Electrochim. Acta* **1992**, *37*, 847−864.
(30) Lewerenz, H. J. Spatial and Temporal Oscillation at Si(111) Electrodes in Aqueous Fluoride-Containing Solution. *J. Phys. Chem. B* **1997**, *101*, 2421−2425.
(31) Chazalviel, J. N.; Fonseca, C.; Ozanam, F. In Situ Infrared Study of the Oscillating Anodic Dissolution of Silicon in Fluoride Electrolytes. *J. Electrochem. Soc.* **1998**, *145* (3), 964.
(32) Chazalviel, J. N.; da Fonseca, C.; Musiani, M.; Ozanam, F. Surface Chemistry during Porous Silicon Formation in Dilute Fluoride Electrolytes. *J. Electrochem. Soc.* **1999**, *147*, 3277−3282.
(33) Schoenleber, K.; Krischer, K. High-Amplitude versus Low-Amplitude Current Oscillations during the Anodic Oxidation of p-Type Silicon in Fluoride Containing Electrolytes. *ChemPhysChem* **2012**, *13*, 2989.
(34) Liu, D.; Blackwood, D. Mechanism and Dissolution Rates of Anodic Oxide Films on Silicon. *Electrochim. Acta* **2013**, *105*, 209−217.
(35) Miethe, I.; Krischer, K. Ellipsomicroscopic Studies of the Anodic Oxidation of p-type Silicon in Fluoride Containing Electrolytes during Current Oscillations. *J. Electroanal. Chem.* **2012**, *666*, 1.
(36) Yahyaoui, F.; Dittrich, T.; Aggour, M.; Chazalviel, J.-N.; Ozanam, F.; Rappich, J. Etch Rates of Anodic Silicon Oxides in Dilute Fluoride Solutions. *J. Electrochem. Soc.* **2003**, *150*, B205−B210.
(37) Nayfeh, A. N.; Mook, D. *Nonlinear Oscillations*; John Wiley & Sons: 1979.
(38) Ozanam, F.; Chazalviel, J.-N.; Radi, A.; Etman, M. Resonant and Nonresonant Behavior of the Anodic Dissolution of Silicon in Fluoride Media: An Impedance Study. *J. Electrochem. Soc.* **1992**, *139* (9), 2491−2501.
(39) Ozanam, F.; Blanchard, N.; Chazalviel, J.-N. Microscopic, Self-Oscillating Domains at the Silicon Surface During Its Anodic Dissolution in a Fluoride Electrolyte. *Electrochim. Acta* **1993**, *38*, 1627−1630.